Keywords: PUMPED-STORAGE POWER STATIONS, DAY-AHEAD ELECTRICITY MARKET, STOCHASTIC OPTIMIZATION

A Nonlinear Hybrid Approach for the Scheduling of Merchant Underground Pumped Hydro Energy Storage

Jean-François Toubeau [1*], Sergei Iassinovski [2], Emmanuel Jean [2], Jean-Yves Parfait [2], Jérémie Bottieau [1], Zacharie De Grève [1], and François Vallée [1]

[1] Department of Electrical Engineering, University of Mons, 31, Boulevard Dolez, Mons, Belgium
[2] Multitel Innovation center, 2, Rue Pierre Et Marie Curie, Mons, Belgium
[*] Jean-Francois.TOUBEAU@umons.ac.be

Abstract: As a result of the increased penetration of stochastic renewable generation, power systems have a growing need of flexibility for compensating real-time mismatches between production and consumption of electricity. This flexibility can be efficiently provided by underground pumped hydro energy storage (UPHES), a new solution where end-of-life quarries or mines are rehabilitated as natural reservoirs. However, the operation of UPHES is significantly different from existing facilities, and is characterized by multiple nonlinear effects with fast dynamics mainly arising from the complex geometry of the unit, and water exchanges between the porous reservoirs and their surrounding aquifers. This paper aims thus at integrating these complex effects within the co-optimization of a UPHES system in the European day-ahead energy and reserve markets. To that end, we leverage a hybrid iterative approach combining an optimization tool with an advanced simulation model. The results from a real-world case study demonstrate that accurately considering these nonlinear effects is a key component to fully extract the economic potential of merchant UPHES, and suggest that the proposed tool offers an effective solution for the scheduling of UPHES owners.

1. Nomenclature

Sets and indexes

$t \in T^{\text{opt}}$	Time steps of the optimization tool
$\tau \in T^{\text{sim}}$	Time steps of the simulation model
$\omega \in \Omega$	Stochastic scenarios
$h \in H$	UPHES units
$r \in R$	Operating reserve products
$R^{+} \subseteq R$	Upward reserve products
$R^{-} \subseteq R$	Downward reserve products

Decisions variables (Step 1)

e_t^{DA}	Energy exchanged on the day-ahead market, MWh
$res_{t,r}$	Total reserve capacity allocated in reserve category r, MW
$res_{h,\omega,t,r}^{\text{P}}$	Allocated reserve in pump (P), MW
$res_{h,\omega,t,r}^{\text{T}}$	Allocated reserve in turbine (T), MW
$p_{h,\omega,t}^{\text{P}}$, $p_{h,\omega,t}^{\text{T}}$	Output power in pump (P) and turbine (T) modes, MW
$z_{h,\omega,t}^{\text{P}}$, $z_{h,\omega,t}^{\text{T}}$	Binary variables indicating the pump (P) and turbine (T) status.
$soc_{h,\omega,t}$	State-of-charge (energy content), MWh
$c_{h,\omega,t}^{\text{op}}$	Operating costs, €
$c_{h,\omega,t}^{\text{SU,P}}$, $c_{h,\omega,t}^{\text{SU,T}}$	Start-up costs in pump (P) and turbine (T) modes, €
$c_{h,\omega,t}^{\text{SD,P}}$, $c_{h,\omega,t}^{\text{SD,T}}$	Shut-down costs in pump (P) and turbine (T) modes, €

State variables (Step 2)

$p_{h,\tau}^{\text{P,res}}$, $p_{h,\tau}^{\text{T,res}}$	Actual power in pump (P) and turbine (T) modes, accounting for the real-time activation of reserves, MW
$h_{h,\tau}^{\text{low}}$, $h_{h,\tau}^{\text{up}}$	Water level in the lower/upper basin, m
$h_{h,\tau}^{\text{net}}$	Net hydraulic head, m
$h_{h,\tau}^{\text{loss}}$	Penstock head losses, m
$v_{h,\tau}^{\text{low}}$, $v_{h,\tau}^{\text{up}}$	Water volume in the lower/upper basins, m^3
$q_{h,\tau}^{\text{P}}$, $q_{h,\tau}^{\text{T}}$	Water flow rates in pump (P) and turbine (T) modes, m^3/s
$q_{h,\tau}^{\text{low,grd}}$, $q_{h,\tau}^{\text{up,grd}}$	Groundwater flows in the lower/upper reservoirs, m^3/s

Functions

$f_h^{\text{UPC,P}}$, $f_h^{\text{UPC,T}}$	Unit performance curves in pump (P) and turbine (T) modes
f_h^{low}, f_h^{up}	Geometry-dependent function of water levels in the lower/upper reservoirs with respect to water volumes
$f_{1,h}^{\text{low,grd}}$, $f_{2,h}^{\text{low,grd}}$	Groundwater interactions between the phreatic table and the lower reservoir
$f_{1,h}^{\text{up,grd}}$, $f_{2,h}^{\text{up,grd}}$	Groundwater interactions between the phreatic table and the upper reservoir

Fixed parameters

Δt, $\Delta \tau$	Time resolution of the optimization tool [0.25 h], and simulation model [10 s]
π_{ω}	Probability of occurrence of scenario ω
λ_r^{res}	Price for availability of reserve capacity in reserve category r, €/MW
$\lambda_{\omega,t}^{\text{DA}}$	Electricity price in the day-ahead market, €/MWh
$H^{\text{low,grd}}$, $H^{\text{up,grd}}$	Height of the groundwater (phreatic) table surrounding the lower/upper basin, m
$C_h^{\text{SU,P}}$, $C_h^{\text{SU,T}}$	Start-up costs in pump (P) and turbine (T) modes, €

$C_h^{SD,P}, C_h^{SD,T}$	Shut-down costs in pump (P) and turbine (T) modes, €

Parameters varying among iterations

$\underline{P}^{P}_{h,\omega,t}, \overline{P}^{P}_{h,\omega,t}$	Minimum/maximum safe output power in pump (P) mode, MW
$\underline{P}^{T}_{h,\omega,t}, \overline{P}^{T}_{h,\omega,t}$	Minimum/maximum safe output power in turbine (T) mode, MW
$\eta^{P}_{h,\omega,t}, \eta^{T}_{h,\omega,t}$	Efficiency of the UPHES system in pump (P) and turbine (T) modes
$\underline{SOC}_{h,\omega,t}$	Lower bound of state-of-charge, MWh
$\overline{SOC}_{h,\omega,t}$	Upper bound of state-of-charge, MWh
$SOC^{target}_{h,\omega}$	Targeted state-of-charge, MWh

2. Introduction

To achieve a more sustainable and less carbon-intensive system, the electricity generation increasingly relies on renewable energy sources, mainly wind and solar. In order to efficiently hedge against the variability and uncertainty of these resources, there is a growing need of flexibility in power systems that can be provided by pumped hydro energy storage (PHES) due to their ability to quickly and cost-effectively respond to imbalances between generation and consumption. PHES plants can indeed store large amount of energy with low operating costs, and recent progresses in power electronics enable these units to widen their output range through a variable-speed operation in both pump and turbine modes [1].

However, the potential of conventional PHES installations is constrained by the necessity to have large available areas as well as a minimum height difference between reservoirs. By contrast, new solutions, in which the reservoirs are located into the ground, e.g. when end-of-life mines or quarries are exploited as natural basins for saving civil engineering expenses, are viable alternatives in flat regions. Such underground PHES (or UPHES) have very limited impacts on landscape, vegetation and wildlife, and can be easily dismantled at the end of their service with a very low ecological footprint. The potential in the Walloon Region in Belgium (which has no significant vertical drop) has been estimated at 815 MW for 5000 MWh, distributed on 76 operable sites [2].

One of the main difficulties related to the scheduling of traditional PHES arises from the need to model the nonlinear pump/turbine performance curves [3], which characterize the relationship among the output power (MW), the water discharge flow (m^3/s), and the net head between both reservoirs (m). To account for these complex water-power conversion curves (and thus to obtain a feasible and realistic UPHES dispatch), researchers have deployed a wide range of techniques. Dynamic programming has been tested but its practical application is hampered due to the curse of dimensionality [4], [5]. As an alternative, Lagrangian relaxation has been applied in [6], but was associated with convergence issues. Then, a nonlinear programming model with some simplified assumptions is proposed in [7]. However, such a nonlinear formulation is intrinsically very complex to solve, and its applicability is limited to small-sized problems [8]. Metaheuristics-based algorithms have also been presented, but such algorithms are not efficient in high-dimensionality in the presence of binary decision variables [9], [10]. Recently, piecewise linear approximation-based formulations, which rely on mixed-integer linear programming (MILP), gained a lot of attention [11]-[16]. Reaching an acceptable approximation of the original nonlinear function may necessitates to considerably increase the number of linear segments. To avoid the associated tractability issues, approximation errors are then inevitably encountered, and may lead to infeasible solutions [17]. This problem is exacerbated for underground plants. Indeed, in addition to the pump/turbine performance curves, the UPHES operation is also governed by additional nonlinearities. The latter mainly arise from (i) the (potentially intricate) geometry of the natural cavities used as reservoirs, and (ii) the water exchanges between the porous reservoirs and their surrounding aquifers, e.g. when the waterproofing work of such cavities is not feasible or uneconomical [18].

In the context of deregulated electricity markets, where the UPHES owner aims at maximizing its revenues, disregarding these nonlinear dependencies may lead to suboptimal solutions that do not fully extract the UPHES economic value, or even to infeasible scheduling (resulting in severe imbalance penalties). Modeling all these nonlinear effects within the UPHES scheduling problem requires a great computational effort (especially in the context of aggregation of several assets optimized over a multi-step ahead horizon in an uncertain environment). Therefore, we propose to decompose the problem into two complementary modules, i.e. a simplified optimization tool and an advanced simulation model of UPHES plants, which are embedded within an iterative learning procedure. Such iterative schemes have already been studied (for different purposes) in the literature. In [19], the coordination between medium and short terms is ensured through a feedback loop where the short-term scheduling is used as a constraint to be added into the mid-term strategy. A similar approach has been proposed in [20] to properly represent the performance curves of head-sensitive plants. Each iteration solves the PHES scheduling using a fixed head, which is successively updated until convergence. Outcomes tend to demonstrate that the model is suitable for scheduling real hydro chains. However, as highlighted in [21], depending on the design of the updating strategy, the algorithm did not converge in some cases, which is why they propose a new nonlinear programming based model. More generally, the suitability of this type of iterative approaches has been questioned in [22]-[23] since they are empiric and case-dependent, with no guarantee that the convergence can be achieved.

Nonetheless, such an iterative "optimization-simulation" methodology is very useful for our application since, in contrast to other approaches [4]-[17], the simulation model is able to fully represent the quick dynamics inherent to the UPHES operation (e.g. due to groundwater exchanges). Moreover, the iterative nature of the method allows to better manage the simulation time (the algorithm can be stopped at any iteration, and we can then use the approximated solution given by the simplified optimization). Finally, regarding this convergence issue, we develop a strategy to determine (ex-ante) the best learning rates between two iterations, and it is empirically observed that the proposed scheme is suitable for our case study.

The main contribution of this work is to thus to analyze the (hydraulic, electro-mechanical and geological

constraints) UPHES constraints, and take into full consideration these (nonlinear) characteristics within the day-ahead UPHES scheduling (i.e. the joint participation in energy, reserve and balancing markets). To that end, we rely on an iterative process, in which decisions are first optimized with a quarter-hourly time step, using a simplified (mixed-integer linear) formulation that can be efficiently solved. Then, a holistic simulation model, encompassing all nonlinear aspects with a high time resolution (10 seconds), is used to evaluate the resulting UPHES scheduling. If the simulation model identifies inaccuracies in the optimized scheduling (such as a violation of water levels within reservoirs), a feedback adjustment under the form of tightened constraints integrated within the simplified optimization is carried out, and the procedure is reiterated until reaching a feasible solution.

The proposed architecture is independent of the underlying tools used for the optimization (scenario-based, robust, chance-constrained formulations, etc.), and for the UPHES simulator. The procedure is therefore very robust to changes in the portfolio configuration (e.g. if the UPHES aggregator integrates new units such as to be considered as a price-maker instead of price-taker) as well as easily adaptable in case of evolutions of the market regulation policy. Results from a Belgian case study highlight that accurately considering nonlinear effects is a key component to extract the full economic potential of UPHES units, and suggest that the proposed hybrid tool is an effective approach to achieve this goal.

The paper is organized as follows. First, we describe (in Section 3) the specificities of underground PHES plants, and how they differ from traditional facilities, with a particular focus on the associated modeling challenges. Based on these considerations, the sequential approach to solve the UPHES scheduling problem is presented in Section 4, along with the design and sizing of each of its constitutive blocks. Section 5 then analyses the practical value of the optimization tool by means of relevant case studies. Finally, conclusions and perspectives are exposed.

3. Underground UPHES operation

As depicted in Fig. 1, a UPHES plant is composed of two reservoirs, located at different height levels, which are coupled through a hydraulic machine (a reversible Francis pump-turbine in the present study). The pump-turbine is linked to an electrical machine (operating as a generator when the unit is in turbine mode, and as a motor when the unit is pumping water), which is connected to the grid.

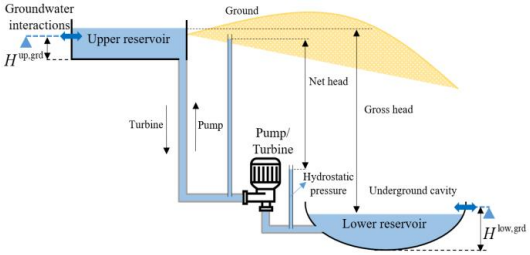

Fig. 1. *Typical underground pumped hydro energy storage (UPHES) system*

The UPHES efficiency in both pump and turbine modes, i.e. water flow requirements to yield a given output power, is a complex function that also depends on the net head value (since the latter defines the pressure conditions across the hydraulic machine). As the head increases, the volume of water required for a given power is reduced. The resulting (three-dimensional) nonlinear relationships in pump (P) and turbine (T) are referred to as unit performance curves (1)-(2).

$$p_t^{\mathrm{P}} = \rho_{water} \cdot g \cdot q_t^{\mathrm{P}} \cdot h_t^{\mathrm{net}} \cdot \eta_t^{\mathrm{P}}\left(q_t^{\mathrm{P}}, h_t^{\mathrm{net}}\right) \ \forall t \quad (1)$$

$$p_t^{\mathrm{T}} = \rho_{water} \cdot g \cdot q_t^{\mathrm{T}} \cdot h_t^{\mathrm{net}} \cdot \eta_t^{\mathrm{T}}\left(q_t^{\mathrm{T}}, h_t^{\mathrm{net}}\right) \ \forall t \quad (2)$$

where ρ_{water} is the density of water (1000 kg/m³), g is the gravitational acceleration (9.81 m/s²), q is the water flow (m³/s), h^{net} is the net head (m), and η refers to the system efficiency (which itself depends on the net head and water flow, and includes losses in the hydraulic machine, the variable-speed drive and the electrical generator).

Additionally, the net head value also influences the stability margins of the pump-turbine. Indeed, traditional hydraulic machines are characterized by forbidden zones (the pump is technically limited to a single working point), in which their safe operation is not guaranteed due to undesired flow phenomena that lead to severe erosion of the machinery. To extend this limited UPHES flexibility, one

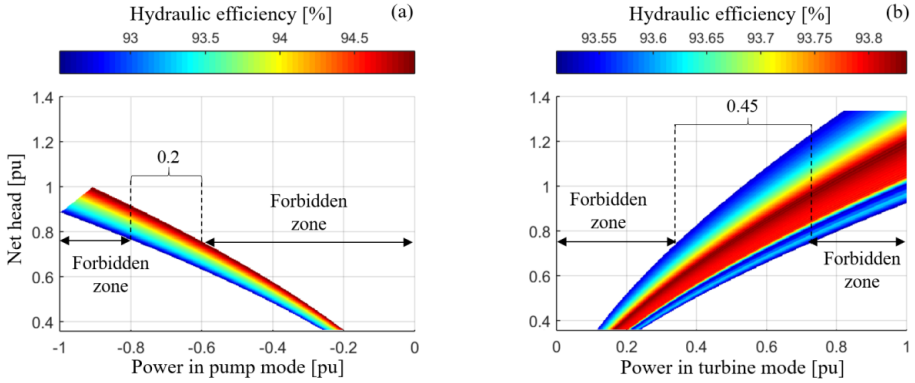

Fig. 2. *Head-dependent UPHES operation in pump (a) and turbine modes (b), where the forbidden (unstable) zones are indicated by the white areas, and the iso-efficiency curves are differentiated through color bar*

solution is to rely on variable speed drives. Practically, this technology allows increasing the available power range, i.e. extent low and high capacity levels where cavitation and/or mechanical vibrations can occur.

Overall, these head effects, i.e. the nonlinear water-power conversion functions and the safe operating ranges (in term of output power), are illustrated in Fig. 2 for a typical reversible variable-speed Francis machine [24]. It can be seen that the range of allowed power is respectively around 20 % and 45 % in pump and turbine modes for head values between 0.7-0.9 pu. Increasing the net head allow to reach higher power values, thereby shifting the safe operation zone (which will impact market decisions).

In parallel, two additional (nonlinear) dependencies inherent in the UPHES operation need to be considered.

Firstly, the geometry of the reservoirs depends on the topological conditions and can potentially take any complex form (e.g. sandstone quarries are traditionally shaped like truncated pyramids). Such geometries result in highly nonlinear relationships between the water volumes stored in the reservoirs and the corresponding net head value.

Secondly, UPHES units may interact with the surrounding aquifers due to natural permeability of the reservoirs. In this way, when the water level in the reservoir is lower than the surrounding groundwater table, groundwater infiltrates (flows in) by leaking through the reservoir walls, whereas groundwater flows out in the opposite situation. These water interactions are quite complex (dependent on hydrogeological dynamics), and are constantly affecting the energy capacity of the site (since the water volumes are varying even when the unit is not in operation). It is very important to emphasize that both the direction and the flow of groundwater exchanges vary endogenously with respect to the water volumes within reservoirs. They differ thus from exogenous water flows (originating from rainfall, snowmelt, natural evaporation, etc.) that can be independently forecasted.

Properly modeling these effects (in order to rely on an accurate evolution of the system state over time) is a challenging task, not only regarding the development of efficient and representative mathematical equations but also regarding the quick dynamics associated with water levels variations (that necessitates a model with a high time resolution). However, this task is essential to ensure that the UPHES model leads to a reliable, feasible operating schedule and, thus, a profit-maximizing market participation.

4. Methodology

In this Section, we formulate the day-ahead operational scheduling problem (i.e. quarter-hourly power output dispatch) faced by an operator of UPHES plants. The price-taker operator maximizes its profit through a joint participation in the day-ahead energy and reserve markets, while considering the real-time balancing market outcomes through scenarios of the activation of reserves in real-time. However, accurately representing the operation of traditional PHES involves high computational requirements [25]. Here, the additional complexity associated with exploiting underground cavities as reservoirs is addressed using the iterative hybrid approach presented in Fig. 3. The principle is to split the modeling complexity (arising from all nonlinear effects) between a simplified optimization tool and an advanced simulation model.

Once uncertainties have been characterized (Step 0 described in Section 4.1), the scheduling strategy is optimized using a simplified (stochastic mixed-integer linear) formulation that can be efficiently solved with off-the-shelf solvers (Step 1 described in Section 4.2). The daily horizon is divided into 96 quarter-hourly periods. At this stage, nonlinear effects (i.e. head dependencies, groundwater exchanges and geometry of the reservoirs) are simplified to avoid both modeling and tractability issues associated with a single mathematical formulation.

Each of the resulting scenario-dependent UPHES schedules (power profiles) is thereafter integrated into a simulation model encompassing hydraulic, electro-mechanical and geological constraints (Step 2 described in Section 4.3). This simulator emulates the actual nonlinear UPHES operation with a high time-resolution (10 seconds to fully consider variations in the operating conditions), which yields the complete system state (hydraulic efficiencies, water volumes in each reservoir, net head, etc.) at each time step. Hence, the simulator can thus highlight whether the decisions (obtained in Step 1) lead to infeasible schedules or are based on unrealistic parameters that can mislead the solver towards a suboptimal point. In such cases, more informed (i.e. relaxed) constraints are introduced in the optimization (Step 1) through a feedback mechanism (Step 3 described in Section 4.4), and the procedure (Steps 1-2-3) is iterated until convergence is achieved.

However, the heuristic nature of the procedure makes it difficult to guarantee the convergence of the algorithm, and hence the optimality of the final solution. The

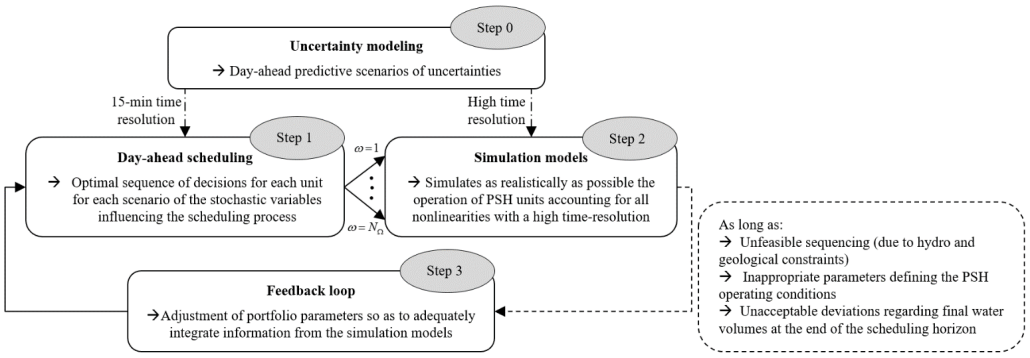

Fig. 3. *Iterative hybrid approach for the day-ahead UPHES scheduling*

possibility of not reaching convergence is alleviated in the control loop (Sections 4.4 and 5.1) by relying on smooth steps between iterations. Then, the global optimum can be better approximated by setting up a multi-start local search algorithm consisting in launching the first optimization (Step 1) under different initial configurations of UPHES parameters. The proposed hybrid sequential tool can then be used (in parallel to keep the computational time in the same range) for the different starting points. Each initial point may potentially lead to a different solution, resulting overall in a higher probability to reach the global optimum, provided that the search space is well covered.

4.1. Step 0: Uncertainty characterization

The quality of the UPHES scheduling depends on the quality of the scenarios representing the sources of uncertainty, i.e. day-ahead market prices (Step 1) and the real-time activation of operating reserves (Step 2). In Step 1, the predictive scenarios ω are generated with a time resolution of 15 minutes (i.e. 96 sequential values over the next day), whereas a smaller time step (down to 10 seconds) is used in the simulation model (Step 2) in order to properly represent the variability of the activation of reserves.

The scenarios are here predicted with the two-stage procedure presented in [26]. Firstly, multivariate probabilistic forecasts (under the form of densities) are generated for each time step of the scheduling horizon using recurrent neural networks [27]. Secondly, a copula-based sampling strategy (from the forecasted densities) is implemented to obtain time trajectories that embody both the temporal information of individual variables (e.g. autocorrelation structure, regime switching, etc.) as well as the cross-variable dependencies (statistical relationships between uncertain variables).

Both the optimization (Step 1) and the simulation (Step 2) are fed and guided by these scenarios, thereby robustifying the UPHES scheduling with respect to the different sources of uncertainty. It should be noted that, since the time granularity differs between optimization and simulation models, we need to ensure the coherence of the scenarios. This is achieved by aggregation/disaggregation mechanisms where the 10 seconds scenarios are averaged into a single quarter-hourly value, while 15 minutes values are simple duplicated within each 10 seconds interval.

4.2. Step 1: Day-ahead UPHES scheduling

The considered market structure arises from the European energy-only and reserve capacity markets, which are cleared sequentially through independent auctions [28]. As represented in Fig. 4, the reserve capacity is cleared on a daily basis, shortly before the energy market.

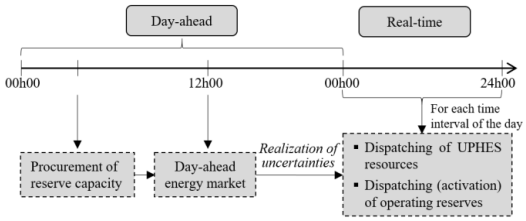

Fig. 4. *Decisions sequences in European market structure*

Considering the short delay between the clearing of both market floors and the strong link between arbitrage and reserve opportunities, the UPHES participation in these day-ahead markets is considered as a single stage problem. By incorporating the UPHES real-time dispatch into the decision process, the resulting profit-maximization problem is formulated as a two-stage stochastic problem [29]-[30].

In the first stage, facing future uncertainties, the UPHES operator has to decide for the 24 hours of the following day on the optimal bidding strategy to adopt in the day-ahead energy e_t^{DA} and reserve $res_{t,r}$ markets (*here-and-now* decisions). Energy prices are uncertain, and thereby modeled via N_Ω different scenarios weighted in accordance with their probability π_ω of occurrence. The price of reserve capacity, however, is treated as a constant parameter that does not vary throughout the day. Hence, the second stage of the model corresponds to intraday operation that aims at avoiding energy imbalances while providing the energy requested for operating reserves. These second-stage decisions (output power of UPHES plants) can be adjusted according to the realization of uncertainties, and differ between scenarios.

The profit Φ^{A} of the UPHES (3) depends on: (i) the revenues for the availability (capacity) of operating reserves over the 24 hours of the scheduling horizon, (ii) the revenues associated with energy arbitrage (sell electricity when prices are high, and purchase at low prices) in the day-ahead energy market, and (iii) the operating costs of the units. In this mixed-integer linear program (MILP) formulation, the participation in the reserves is budget-neutral, i.e., the expected revenues are offset by the UPHES operating costs.

$$\max \Phi^{\mathrm{A}} = \sum_{t\in T}\left[\underbrace{\sum_{r\in R} 24\lambda_r^{\mathrm{res}} \sum_{h\in H} res_{t,r}}_{\text{(i)}} + \sum_{\omega\in\Omega}\pi_\omega\left[\underbrace{\lambda_{\omega,t}^{\mathrm{DA}} e_t^{\mathrm{DA}}}_{\text{(ii)}} - \underbrace{\sum_{h\in H} c_{h,\omega,t}^{\mathrm{op}}}_{\text{(iii)}}\right]\right] \quad (3)$$

This optimization is subject to a number of constraints. First, we ensure that the energy sold and bought in the day-ahead electricity market is actually delivered at the corresponding delivery period (4):

$$e_t^{\mathrm{DA}} = \Delta t \sum_{h\in H}\left(p_{h,\omega,t}^{\mathrm{T}} - p_{h,\omega,t}^{\mathrm{P}}\right) \quad \forall \omega, t \quad (4)$$

The flexibility of the UPHES units can be valued in the reserve market, by offering capacity in the different products $r \in R$ over the scheduling horizon (5). Upward reserve capacity can be supplied either by increasing the turbine output power or by reducing the pump contribution. Similarly, downward reserves are provided by lowering the turbine power or by increasing the pump output power [31]:

$$res_{t,r} = \sum_{h\in H}\left(res_{h,t,r}^{\mathrm{T}} + res_{h,t,r}^{\mathrm{P}}\right) \quad \forall t, r \quad (5)$$

Then, as presented in Section 3 (see Fig. 2), UPHES plants are characterized by forbidden operating zones (in term of output power), defined by stability and cavitation limits of the hydraulic pump/turbine machine. These restricted zones (which are often disregarded in the literature) lead to a discontinuous operating domain that requires two binary variables $z_{h,t}^{\mathrm{P}}$ and $z_{h,t}^{\mathrm{T}}$ to discriminate operation modes, i.e. pump (P), turbine (T) and idle, at each time step t.

$$z^{\mathrm{T}}_{h,\omega,t} + z^{\mathrm{P}}_{h,\omega,t} \le 1 \quad \forall h,\omega,t \qquad (6)$$

In addition, these safe UPHES operating ranges must account for the capacity margins offered to reserves (7)-(10). Specifically, the UPHES power may not be simultaneously allocated to provide both energy arbitrage and regulation services (i.e. the activation of the scheduled reserve capacity must be always guaranteed). In this simplified model (Step 1 of the hybrid tool), head effects (and thus the complex geometry of reservoirs) are neglected, so that both the safe operation range (minimum and maximum output power) and the UPHES efficiency are treated as constant parameters over each time step $t \in T^{opt}$ of the scheduling horizon.

$$p^{\mathrm{P}}_{h,\omega,t} \ge z^{\mathrm{P}}_{h,\omega,t}\,\underline{P}^{\mathrm{P}}_{h,\omega,t} + \sum_{r\in R^{+}} res^{\mathrm{P}}_{h,t,r} \quad \forall h,\omega,t \qquad (7)$$

$$p^{\mathrm{P}}_{h,\omega,t} \le z^{\mathrm{P}}_{h,\omega,t}\,\overline{P}^{\mathrm{P}}_{h,\omega,t} - \sum_{r\in R^{-}} res^{\mathrm{P}}_{h,t,r} \quad \forall h,\omega,t \qquad (8)$$

$$p^{\mathrm{T}}_{h,\omega,t} \ge z^{\mathrm{T}}_{h,\omega,t}\,\underline{P}^{\mathrm{T}}_{h,\omega,t} + \sum_{r\in R^{-}} res^{\mathrm{T}}_{h,t,r} \quad \forall h,\omega,t \qquad (9)$$

$$p^{\mathrm{T}}_{h,\omega,t} \le z^{\mathrm{T}}_{h,\omega,t}\,\overline{P}^{\mathrm{T}}_{h,\omega,t} - \sum_{r\in R^{+}} res^{\mathrm{T}}_{h,t,r} \quad \forall h,\omega,t \qquad (10)$$

Then, limits on the energy content (11) have to be respected at each time step. The state-of-charge (SOC) accounts for energy losses originating from pump and turbine inefficiencies, as well as the impact of activating reserves in real-time. Indeed, when scheduling reserves, one should ensure that sufficient energy is stored in the UPHES (for upward reserves), or that one can store the absorbed energy (for downward reserves). In this formulation, we ensure the robustness of the UPHES scheduling in the worst-case scenario, i.e. in case of full deployment of all reserves in one direction (12)-(13). Furthermore, the final energy content stored at the end of the day is imposed in order to account for the economic value of the energy during following days (14).

$$soc_{h,\omega,t} = soc_{h,\omega,t-1} + \Delta t\left(\eta^{\mathrm{P}}_{h,\omega,t}\,p^{\mathrm{P}}_{h,\omega,t} - \frac{p^{\mathrm{T}}_{h,\omega,t}}{\eta^{\mathrm{T}}_{h,\omega,t}}\right) \quad \forall h,\omega,t \qquad (11)$$

$$soc_{h,\omega,t} + \Delta t\left(\sum_{t'=1}^{t}\sum_{r\in R^{-}} \eta^{\mathrm{P}}_{h,\omega,t'}\,res^{\mathrm{P}}_{h,t',r} + \sum_{t'=1}^{t}\sum_{r\in R^{+}} \frac{1}{\eta^{\mathrm{T}}_{h,\omega,t'}}\,res^{\mathrm{T}}_{h,t',r}\right) \le \overline{\mathrm{SOC}}_h \quad \forall h,\omega,t \qquad (12)$$

$$soc_{h,\omega,t} - \Delta t\left(\sum_{t'=1}^{t}\sum_{r\in R^{+}} \eta^{\mathrm{P}}_{h,\omega,t}\,res^{\mathrm{P}}_{h,t',r} + \sum_{t'=1}^{t}\sum_{r\in R^{+}} \frac{1}{\eta^{\mathrm{T}}_{h,\omega,t'}}\,res^{\mathrm{T}}_{h,t',r}\right) \ge \underline{\mathrm{SOC}}_h \quad \forall h,\omega,t \qquad (13)$$

$$soc_{h,\omega,t=T^{\mathrm{opt}}} \ge \mathrm{SOC}^{\mathrm{target}}_h \quad \forall h,\omega \qquad (14)$$

Finally, operating costs are incorporated (15). These are composed of running costs as well as transition costs, i.e. start-up (16) and shut-down (17) costs in both pump and turbine modes, to properly consider water losses as well as wear and tear of hydraulic and electrical equipment.

$$c^{\mathrm{op}}_{h,\omega,t} = \Delta t C^{\mathrm{run}}_h\left(p^{\mathrm{T}}_{h,\omega,t} + p^{\mathrm{P}}_{h,\omega,t}\right) + c^{\mathrm{SU},i}_{h,\omega,t} + c^{\mathrm{SD},i}_{h,\omega,t},\ \forall h,\omega,t,i \in \{\mathrm{T},\mathrm{P}\} \qquad (15)$$

$$c^{\mathrm{SU},i}_{h,\omega,t} \ge C^{\mathrm{SU},i}_h\left(z^{i}_{h,\omega,t} - z^{i}_{h,\omega,t-1}\right),\ \forall h,\omega,t,i \in \{\mathrm{T},\mathrm{P}\} \qquad (16)$$

$$c^{\mathrm{SD},i}_{h,\omega,t} \ge C^{\mathrm{SD},i}_h\left(z^{i}_{h,\omega,t-1} - z^{i}_{h,\omega,t}\right),\ \forall h,\omega,t,i \in \{\mathrm{T},\mathrm{P}\} \qquad (17)$$

4.3. Step 2: UPHES simulation model

The day-ahead scheduling problem (Step 1) is formulated with modeling approximations regarding head effects and groundwater exchanges. To avoid suboptimal or even infeasible outcomes, the optimization is thus embedded within an iterative approach (Fig. 3), in which a simulation model (Step 2) is used to validate the UPHES scheduling decisions. In this way, at the end of Step 1, each of the N_Ω UPHES power profiles are evaluated using the simulation model, which takes into full consideration the impact of all geo-mechanical, hydrogeological and electrical parameters, thereby yielding an accurate evolution of the system state for each time step of the scheduling horizon. The resulting model of the UPHES operation is implemented in RAO (Resource-Action-Operation), an object-oriented language dedicated to the modeling and simulation of complex systems [32]. Practically, for each scenario ω, the procedure (18)-(27) is sequentially applied for each 10 seconds interval. All nonlinear functions (18), (19), (22), (23), (24) and (25) are encoded as arrays, which allows representing all effects empirically with a high accuracy without mathematical approximations.

First, the actual UPHES output power is computed by accounting for the activation of reserves (in accordance with the scenarios $\omega \in \Omega$ defined in Step 0). Then, the characteristics of the hydraulic pump/turbine machine can be used to identify the corresponding water flows. Indeed, as described in Section 3 (and illustrated in Fig. 2), hydraulic machines are constrained by three-dimensional nonlinear relations, i.e. unit performance curves (UPC), linking the net head, the output power, and the unit outflow. At each time period τ of the simulation horizon, the water flow in both pump (18) and turbine (19) modes are computed as follows:

$$q^{\mathrm{P}}_{h,\tau} = f^{\mathrm{UPC,P}}_h\left(p^{\mathrm{P,res}}_{h,\tau}, h^{\mathrm{net}}_{h,\tau-1}\right) \quad \forall h,\tau \qquad (18)$$

$$q^{\mathrm{T}}_{h,\tau} = f^{\mathrm{UPC,T}}_h\left(p^{\mathrm{T,res}}_{h,\tau}, h^{\mathrm{net}}_{h,\tau-1}\right) \quad \forall h,\tau \qquad (19)$$

Moreover, these performance curves are also exploited to identify the actual efficiency values as well as the boundary (safe) power conditions (interface between colored and white areas in Fig. 2), which allows determining the correctness of the parameters used in Step 1.

The water volumes in the upper (20) and lower (21) reservoirs (reflecting the UPHES energy content), are not only affected by the charge and discharge decisions across the scheduling horizon, but also by interactions with the surrounding aquifers. After computing these water volumes, it is checked whether they comply with the limitations imposed by the UPHES sizing. If not, it means that the power scheduling (of Step 1) is infeasible, and energy bounds in (12)-(13) are then updated in the next iteration of the hybrid tool (see Section 4.4).

$$v^{\mathrm{up}}_{h,\tau} = v^{\mathrm{up}}_{h,\tau-1} + \left(q^{\mathrm{P}}_{h,\tau} - q^{\mathrm{T}}_{h,\tau}\right)\Delta\tau + q^{\mathrm{up,grd}}_{h,\tau}\Delta\tau \quad \forall h,\tau \qquad (20)$$

$$v^{\mathrm{low}}_{h,\tau} = v^{\mathrm{low}}_{h,\tau-1} + \left(q^{\mathrm{T}}_{h,\tau} - q^{\mathrm{P}}_{h,\tau}\right)\Delta\tau + q^{\mathrm{low,grd}}_{h,\tau}\Delta\tau \quad \forall h,\tau \qquad (21)$$

Groundwater exchanges, as explained in Section 3, are water flows that vary endogenously with respect to the height difference between the water level in the reservoir and the surrounding phreatic table. These water exchanges are determined using advanced hydro-geological models [33]. In a nutshell, when the water level in the reservoir is lower than the groundwater table, then groundwater infiltrates the reservoir by leaking through the porous walls

(in accordance with f_1 in (22)), whereas some water flows out of the reservoir (in accordance with f_2 in (23)) in the opposite case.

$$q_{h,\tau}^{\text{up,grd}} = \begin{cases} f_{1,h}^{\text{up,grd}}\left(h_{h,\tau-1}^{\text{up}}\right) \text{ if } h_{h,\tau-1}^{\text{up}} > H_h^{\text{up,grd}} \\ f_{2,h}^{\text{up,grd}}\left(h_{h,\tau-1}^{\text{up}}\right) \text{ if } h_{h,\tau-1}^{\text{up}} < H_h^{\text{up,grd}} \end{cases} \quad \forall h,\tau \qquad (22)$$

$$q_{h,\tau}^{\text{low,grd}} = \begin{cases} f_{1,h}^{\text{low,grd}}\left(h_{h,\tau-1}^{\text{low}}\right) \text{ if } h_{h,\tau-1}^{\text{low}} > H_h^{\text{low,grd}} \\ f_{2,h}^{\text{low,grd}}\left(h_{h,\tau-1}^{\text{low}}\right) \text{ if } h_{h,\tau-1}^{\text{low}} < H_h^{\text{low,grd}} \end{cases} \quad \forall h,\tau \qquad (23)$$

Finally, the height of the water column in the upper (24) and lower (25) reservoirs is a function of the water volume in the corresponding reservoir, which depends on the geometry of the natural cavity. Complex geometries thereby result in highly nonlinear functions. Due to friction and turbulence within the penstock, the net head is always lower than the gross head (27). This penstock head loss (26) is usually modeled as a quadratic function of the water flow, whose coefficient depend on the pipe characteristics [34]:

$$h_{h,\tau}^{\text{up}} = f_h^{\text{up}}\left(v_{h,\tau}^{\text{up}}\right) \quad \forall h,\tau \qquad (24)$$

$$h_{h,\tau}^{\text{low}} = f_h^{\text{low}}\left(v_{h,\tau}^{\text{low}}\right) \quad \forall h,\tau \qquad (25)$$

$$h_{h,\tau}^{\text{loss}} = c_h^{\text{loss}}\left(q_{h,\tau}^{\text{T}} + q_{h,\tau}^{\text{P}}\right)^2 \quad \forall h,\tau \qquad (26)$$

$$h_{h,\tau}^{\text{net}} = \underbrace{h_{h,\tau}^{\text{up}} - h_{h,\tau}^{\text{low}}}_{\text{gross head}} - h_{h,\tau}^{\text{loss}} \quad \forall h,\tau \qquad (27)$$

4.4. Step 3: Control loop

The aim of the control loop (Fig. 5) is to drive the iterative procedure towards a converged UPHES state in both optimization and simulation steps.

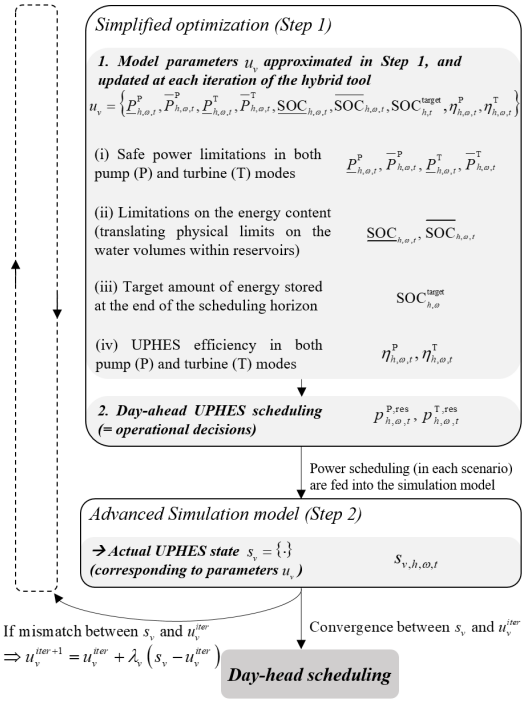

Fig. 5. *Principle of the control loop*

The day-ahead scheduling is carried out (in Step 1) with a simplified model of the UPHES operation. Practically, important state variables (such as the net head and groundwater exchanges) are treated as constant parameters to avoid the associated modeling complexity. Hence, the UPHES power scheduling obtained at the end of this step may be suboptimal in practice, or even infeasible. The resulting UPHES scheduling solution is therefore tested in an advanced simulation model. At the end of this simulation (Step 2), the actual evolution of the UPHES state for each scenario ω is computed, which allows identifying inaccuracies in the UPHES scenario-dependent schedules obtained in Step 1.

When discrepancies between the parameters u_v used in the optimization (Step 1) and the actual UPHES state s_v (Step 2) are observed, these parameters u_v need to be updated with the objective to prevent infeasible schedules in future iterations. Since the parameters s_v may fluctuate (with 10 seconds resolution) within the 15 minutes optimization intervals, the most conservative values s_v are selected to ensure the feasibility of the power scheduling at each point in time. In practice, the UPHES state variables u_v approximated in Step 1, and listed in (28), can be grouped into four different sets.

$$u_v = \{\underbrace{\underline{P}^{\text{P}}_{h,\omega,t}, \overline{P}^{\text{P}}_{h,\omega,t}, \underline{P}^{\text{T}}_{h,\omega,t}, \overline{P}^{\text{T}}_{h,\omega,t}}_{\text{(i)}}, \underbrace{\underline{\text{SOC}}_{h,\omega,t}, \overline{\text{SOC}}_{h,\omega,t}}_{\text{(ii)}}, \underbrace{\text{SOC}^{\text{target}}_{h,\omega}}_{\text{(iii)}}, \underbrace{\eta^{\text{P}}_{h,\omega,t}, \eta^{\text{T}}_{h,\omega,t}}_{\text{(iv)}}\} \qquad (28)$$

First, since head effects are disregarded in Step 1, the safe power limits (i) in both pump and turbine modes are approximated in (7)-(10), and these values need to be adjusted (in accordance with the UPHES state). Similarly, the water levels within reservoirs are not directly modeled, but are represented through the energy content (in MWh). This approximation can lead to infeasible solution (negative water volumes or undesired spillage). When such a case is revealed by the simulation model, the energy limitations (ii) in (12)-(13) are tightened/relaxed in Step 1 to drive the scheduling towards its feasible set in the next iteration. Then, it is also checked whether the amount of energy stored at the end of the scheduling horizon (iii) complies with the targeted value in (14). Finally, the hydraulic efficiency in both pump and turbine (iv) fluctuates over time (according to efficiency curves represented in Fig. 2), which impacts the UPHES optimal scheduling. These parameters are thus refined when deviations between Steps 1 and 2 exceed a given threshold.

In practice, to avoid undesirable diverging oscillations (and guarantee a smooth and efficient convergence of the hybrid tool), the model parameters are adjusted through an iterative learning process of the form:

$$u_v^{iter+1} = u_v^{iter} + \lambda_v\left(s_v - u_v^{iter}\right) \qquad (29)$$

where u_v^{iter} is the value of the model parameter v during iteration *iter* of Step 1, while s_v is the actual value determined by the simulation model, and λ_v is the corresponding learning rate. When $\lambda_v = 1$, it amounts to enforce the output of the simulation model as the new value of the UPHES parameter for the next iteration of the hybrid tool. Such a strategy has shown to give suboptimal results [22], in which diverging oscillations are likely to occur.

In that regard, the performance of the hybrid tool strongly depends on the choice of an appropriate learning rate (i.e. magnitude of the refinement of model parameters at each iteration). An important step consists thus in tuning this learning rate such that the hybrid tool converges quickly and reliably towards a feasible solution. This procedure is performed offline (see Section 5.1), so that it does not hamper the daily operation of the tool.

5. Case study

The methodology is applied to an existing Belgian topology (Maizeret), for which the lower reservoir is a former open pit mine. The surface of both reservoirs (~30.000 m^2) is relatively limited, which incurs significant head variations. The upper reservoir is rectangular-shaped so that (24) is linear, whereas the lower reservoir has a slightly more complex (pyramidal) geometry. The nominal output power of the UPHES is equal to 8 MW in both pump and turbine modes. The energy capacity is of 80 MWh. Throughout this study, it is imposed that the targeted amount of water stored in the upper reservoir at the end of the day is identical to its initial value (i.e. 15 MWh). Practically, this final stored energy can be determined through a medium-term (e.g. week-ahead) analysis [35]. The pump and turbine operating costs are equal to 4 €/MWh, the start-up costs are 5 €, and the shut-down costs are neglected.

Electricity prices in the day-ahead market are modeled from BELPEX data. In terms of operating reserves $r \in R$, frequency containment reserves, FCR (10 €/MW/h), are automatically activated to alleviate momentary frequency deviations. Then, automatic frequency restoration reserves, aFRR (20 €/MW/h), are dispatched to take over the actions of FCR. If the problem persists, the system operator requests the activation of manual frequency restoration reserves, mFRR (5 €/MW/h), which remain online until the situation is resolved. FCR must be fully activated in 0.5 minutes, aFRR in 7.5 minutes and mFRR in 15 minutes.

In what follows, we first focus in Section 5.1 on the sizing of the control loop (i.e. determination of the learning rates within the iterative procedure). In Section 5.2, we analyze the impact the UPHES nonlinear effects on the quality of the day-ahead scheduling, and show the added value of the proposed hybrid tool. In order to focus on the interpretability of results, the procedure is carried out for a single typical day of July. The convergence of the procedure is studied in Section 5.3. Finally, the validity of the approach is evaluated in Section 5.4, where the proposed tool is validated on 8 representative days (one per season with a differentiation between week and weekend days), in which results are compared with those obtained with a genetic algorithm. The scalability is then evaluated with the aggregation of three UPHES plants. For all these simulations, the stochastic MILP optimization (Step 1) is run with $N_\Omega = 5$ scenarios (0.1 % relative optimality gap).

5.1. Design of the control loop

In order to avoid that the outcomes of the hybrid tool diverge at each iteration, the key point lies in the proper selection of the learning rates λ_v in (29). In this work, 4 different learning rates λ_v (v = 1, 2, 3, 4) are used (one for each type of parameters presented in Fig. 5). This sizing is performed in pre-processing, and does not impact the computation time during the daily use of the decision tool.

Firstly, a sensitivity analysis is carried out to analyze the effect of the learning rates on both the convergence and optimality of the solution. The convergence criteria, for each scenario of the global hybrid tool, are the following:

1) Obtain a feasible scheduling (in terms of output power and water volumes within reservoirs).

2) Restrict the relative difference between the final targeted energy content (at the end of the scheduling horizon) and the actual value below 1%, so as not lowering the UPHES economic value for the next days.

3) Restrict the relative difference between values of efficiencies (used in Steps 1 and 2) beneath 1% so that the feasibility and accuracy of the solution is guaranteed.

Practically, the hybrid tool is run for different sets of the 4 learning rates (by relying on a grid search). For each (4-dimensional) point of the grid search, the optimization outcomes are averaged over 8 representative days (one per season, differentiated between week and weekend days), which are generated using [36] with 5 years of historical market data (from 2013 to 2017), in order to properly cover possible scenarios over a typical year. Based on these results, we represent the influence of learning rates (associated with the update of power (i) and energy (ii) limitations) on the convergence speed (Fig. 6a) and final expected profit (Fig. 6b).

Overall, if the learning rate is too small, the convergence of the optimization will necessitate many iterations, which is time-consuming. On the other hand, with an oversized learning rate (significant changes in parameters

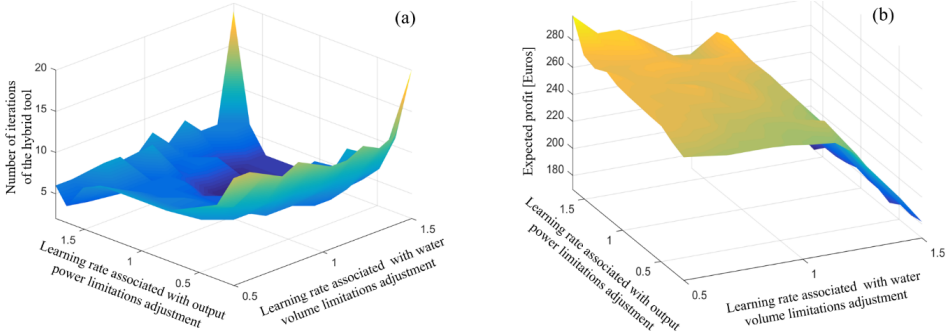

Fig. 6. *Impact of the design parameters of the control loop on the number of iterations of the hybrid tool (a), and on the expected profit (b).*

between two consecutive optimizations), instabilities (divergence) in the learning phase can occur. Furthermore, from Fig. 6b, it is also observed that high learning rates often lead to conservative solutions, resulting in loss of revenues. Indeed, the large step sizes between iterations lead to excessively tightened operating ranges, which prevents the UPHES flexibility to be fully exploited.

Based on these observations, a two-step procedure is implemented to achieve the best trade-off between convergence speed and quality of the final scheduling solution. At the first stage, the different (4-dimensional) sets of learning rates λ_v (among all sets of the grid search) that lead (in average) to the lowest number of iterations are identified. Indeed, different sets of learning rates can result into similar convergence properties (Fig. 6a). Then, for the selected sets, the one that leads to the highest expected profit (best quality of the solution) is chosen (Fig. 6b). Globally, in accordance with [20], we conclude that learning rates between 0.7 and 0.9 lead to the best results.

5.2. Impacts of the UPHES nonlinear effects

In this part, we study the effects of disregarding the nonlinear effects of UPHES units in terms of operational profit and tractability. To that end, the simulations are carried out for a typical day of July with three different formulations, which differ by their level of complexity.

In variant #1, all UPHES nonlinear effects are neglected, including the discontinuous operating domain (due to the forbidden zones of the hydraulic machines) characterized by constraints (7) and (9). Hence, the binary state variables (to discriminate pump-turbine-offline operation modes) are not necessary, and the simplified model (Step 1) boils down to a continuous linear program. Moreover, the hybrid methodology is reduced to a single run of the optimization program (Step 1).

In variant #2, the discontinuous UPHES operating ranges are integrated into the simplified scheduling problem (the formulation is the one presented in Section 4.2). In this variant, the simulator is still not exploited, such that the complex geometry of reservoirs, head dependencies and groundwater exchanges are still neglected.

In variant #3, all nonlinearities are included into the simulator, and the resulting iterative formulation therefore yields the solution of reference.

For each of the three variants, at the end of the day-ahead optimization procedure, the UPHES unit will participate in the day-ahead (energy and reserve) markets in accordance with the outcome of the decision tool. Then, the next day, for variants #1 and #2, it may happen that the UPHES unit is not able to fulfill the schedule in real-time because some nonlinear effects were inaccurately modeled during the decision procedure. In such a case, the unit will stay in its safe operation zone (to avoid damage on the hydraulic machine), and consequently deviate from its balanced position (in the energy market), which will result in financial penalties. Such energy imbalances are penalized at 100 €/MWh. Moreover, the final amount of energy stored at the end of the day may differ from the targeted value. To quantify this effect, the final UPHES energy content is valued at 40 €/MWh. These situations are quantified in Table 1, which includes the total simulation time as well as the ex-ante profit $E(\Phi^{init})$ that is expected at the end of the optimization procedure, and the ex-post profit $E(\Phi^{final})$ that is actually generated after accounting for the imbalance penalties and the economic value of the final stored energy. The last column $E(soc^{final})$ is the amount of energy stored in the upper reservoir at the end of the day.

Table 1 Comparison of formulations of varying complexity in terms of simulation time and profit distribution

	Time	$E(\Phi^{init})$	$E(\Phi^{final})$	$E(soc^{final})$
variant #1	< 1 sec	1395.9 €	273.1 €	11.9 MWh
variant #2	74 sec	1079.6 €	813.4 €	13.3 MWh
variant #3 (reference)	294 sec	873.1 €	873.1 €	15.1 MWh

Results show that, at the end of the optimization, variant #1 expects a profit of 1395.9 €, whereas it will only generate 273.1 € in reality, mainly due to the financial penalties arising from inabilities to fulfill the day-ahead commitment in the energy market. Variant #2 leads to a more cost-effective solution, but at the expense of higher computation times (due to the inclusion of binary variables to model the discontinuous operating ranges). Both variants #1 and #2 do not comply with the targeted amount of energy stored at the end of the time horizon, which will hinder the UPHES strategy for the following days.

In general, ignoring the nonlinear effects during the optimization process results into a systematic error between the expected and actual profits. Such discrepancies are exacerbated when important effects are disregarded. In this way, the difference between ex-post profits in variants #1 and #2 strongly highlights the importance of accurately modeling forbidden zones (7)-(10). Moreover, it should be reminded that the considered UPHES plant is characterized by reservoirs with simple (close to rectangular) geometries. For more complex geometries (such as former mines), head dependencies can be significantly amplified, which will decrease the performance of simplified decision tools. These results thus highlight the importance of developing new nonlinear tools such as the one implemented in this paper.

The solution of variant #2 for the first stochastic scenario is represented in Fig. 7 (for the 86,400 seconds of the day). It can be observed that the schedule is not feasible since the output power profile is often outside its safe operating range. Similarly, when analyzing the evolution of the water level in the upper reservoir, it is observed that water volume violations at the end of the day are also observed (lack of 1.7 MWh of energy). These inaccuracies lead to a loss of profit of 6.84 % in comparison with the reference solution #3 (in which the scheduled energy can be fully delivered in real-time). The solution of variant #3 is achieved after 4 iterations (of around 73.5 seconds).

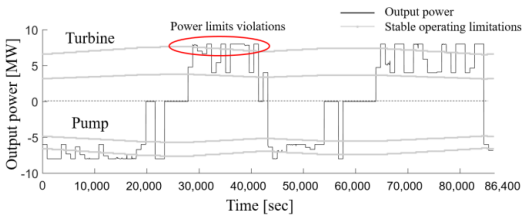

Fig. 7. *UPHES schedule in variant #2 where the nonlinear effects are approximated.*

The final schedule obtained with variant #3 is illustrated in Fig. 8. It can be seen that the proposed hybrid method does not lead to infeasible solutions. Overall, the proposed methodology enables to immunize the scheduling of underground PHES against modeling inaccuracies used for approximating the nonlinear effects of the unit.

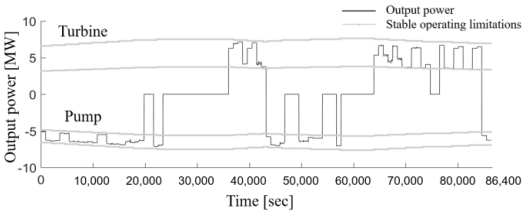

Fig. 8. *UPHES schedule in variant #3 where all nonlinear effects are considered*

More generally, we observe that the UPHES profitability is extracted from the joint participation in energy arbitrage (discharging electricity at high prices, and charging when prices are low) and procurement of reserves. If price spreads in the energy market are not sufficiently important, the UPHES will stay in idle mode since the associated revenues are not sufficient to compensate the UPHES inefficiencies and operation costs. However, such situations are not often encountered in practice due to the additional benefit that can be leveraged from reserves. Providing these operating reserve involves that the UPHES is operating far from the zero output, which results in frequent switches between pump and turbine modes. Interestingly, we also observe that, at the very end of the day, water is pumped into the upper reservoir in order to satisfy the final volume target.

5.3. Convergence of the method

The evolution of the solution (of variant #3) across iterations is illustrated in Table 2. Practically, the evolution of the expected profit is presented, along with those of the 4 types of parameters that need to achieve convergence (which are defined in Section 4.4 and summarized in Fig. 5): (i) the energy (aggregated over the day) that is scheduled outside the safe operating ranges, (ii) the aggregated water volumes violating the reservoirs capacity (in m³), (iii) the deviation with respect to the targeted final value of stored energy (in MWh) as well as (iv) inaccuracies in values used (in Step 1) to define turbine and pump efficiencies (in %).

Table 2 Evolution of the error term across iterations

	$E\left(\Phi^{init}\right)$ [€]	Power limits [MWh]	Water Volumes [m³]	Final Energy [MWh]	η^T [%]	η^P [%]
1	1079.6	8.61	$5.8*10^3$	1.72	1.3	< 1
2	886.8	0	$3.8*10^3$	0	1.3	<1
3	881.3	0	$1.4*10^3$	0	1.2	<1
4	873.1	0	0	0	<1	<1

It is important to notice that, the first iteration of the hybrid tool corresponds to variant #2 (which is characterized by infeasible power and energy schedules, and a loss of 1.7 MWh with respect to the targeted final energy content). It can be seen that, based on this first solution, the implemented iterative procedure allows to smoothly converge (in 4 iterations) towards a feasible and realistic outcome without significantly affecting the UPHES profit. Indeed, the solution is progressively driven towards its feasible range (with no diverging oscillations between iterations). Specifically, after one iteration, the algorithm is already close to a stable solution (i.e. no more power deviations are observed).

5.4. Scalability of the model and benchmark with a meta-heuristic approach

In this subsection, the proposed hybrid approach is applied for the 8 representative days (defined in Section 5.1) in order to analyze more thoroughly the practical applicability of the tool. In parallel, all these cases have been solved by applying a single optimization problem (considering all the linear and nonlinear constraints). To that end, a genetic algorithm is selected since it provides a very general framework and thus serves as a good foundation for comparison. To account for the complex UPHES behavior into the single formulation, the UPHES internal state needs to be accurately represented, leading to some modifications of the (Step 1) decision problem (3)-(17). Practically, the net head, water flows and water volumes within reservoirs must be explicitly incorporated as decision variables into the model. First, the constraints (11)-(14) related to the UPHES energy content are replaced by (20)-(23), which directly integrate water volumes, taking into account groundwater exchanges (22)-(23). The latter, which are depicted in Fig. 9 for an actual Belgian cavity (located in Maizeret), are approximated by third degree polynomials. In addition, it is necessary to accurately model both head variations (which depend on the geometry of reservoirs) using (24)-(27), and unit performance curves (18)-(19). Finally, since genetic algorithms cannot handle simultaneously integer variables and equality constraints, the latter need to be transformed into two inequality constraints. Overall, the optimization is performed with a 15-minutes time step (higher dynamics are disregarded) to keep the problem tractable, hence, infeasibilities can still occur.

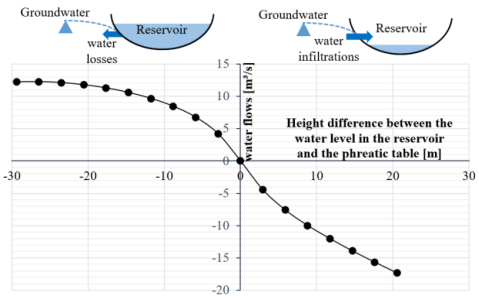

Fig. 9. *Groundwater exchanges for the lower reservoir of the considered Belgian site*

The outcomes given by the three variants and the genetic algorithm (GA) are summarized in Table 3. We focus on the (ex-ante) profit expected at the end of the optimization, and the (ex-post) actual revenues (decomposed into the minimum, average and maximum values for the 8 representative days).

Table 3 Comparison of different formulations in terms of simulation time and profit distribution

	Average ex-ante profit	Average ex-post profit	Min. ex-post profit	Max. ex-post profit
variant #1	1513.2 €	345.7 €	273.1 €	402.3 €
variant #2	1271.6 €	844.6 €	813.4 €	912.0 €
variant #3 (reference)	963.0 €	963.0 €	873.1 €	1104.6 €
GA	1118.5 €	902.2 €	799.1 €	988.9 €

It is important to point out that the proposed tool (variant #3) achieves convergence in all the tested scenarios, with a number of iterations varying between 2 and 5 (resulting in a simulation time of maximum 8 minutes). Those results were obtained with the tight tolerance parameters (convergence criteria) described in Section 5.1, which tends to prove the validity of the approach.

As expected, meta-heuristics are not efficient in high-dimensionality, especially in the presence of integer decision variables (and thus generate lower revenues). The increase in revenue obtained with respect to the genetic algorithm ranges from 2.1% to 10.4%, with an average value of 6.3%, which corresponds to 60.8 € per day (i.e. around 22,200 € per year). However, since nonlinear effects are better represented, the genetic algorithm leads to a lower mismatch (than variants #1 and #2) between the value of the objective function and the actual UPHES revenues.

In general, summer months are characterized by lower price spreads compared to other months of the year. Consequently, the mean yearly profits (in Table 3) are higher than those observed for the month of July. Moreover, we see that variant #2 often yields a good initial policy, so that the proposed model (variant #3) can exploit this initial solution to efficiently improve (at each iteration) the operational decisions (until convergence). Interestingly, we also observe that, for 1 scenario, variant #2 generates slightly higher revenues than the proposed hybrid tool. This can be explained by the fact that, in this particular case, the hybrid approach leads to an overly conservative outcome, i.e. loss of revenues that exceeds the financial penalties associated with the aggressive strategy of variant #2.

Finally, the scalability of the methodology is studied through a pool-commitment of 3 similar UPHES units (for the typical day of July). If the nonlinear effects had to be added directly to this formulation, the problem would quickly become intractable. However, for the hybrid tool, the variant #3 still requires 4 iterations to obtain the optimal solution, which shows that the convergence speed is not affected by the portfolio effect (aggregation of assets). The total simulation time, however, now reaches 25 minutes, due to the resulting increased complexity of the MILP optimization problem (Step 1). It should be noted that the calculation load of the RAO simulation model (Step 2) is not analyzed since it takes less than 1 second.

6. Conclusions

In this paper, we propose a methodology to robustify the scheduling problem faced by UPHES owners against the approximation errors arising when representing the nonlinear operation of these units. Indeed, we highlight that disregarding the nonlinear behaviors may mislead the UPHES operator into believing that the scheduling obtained at the end of the optimization is efficient and reliable, while it may actually lead to infeasible and sub-optimal strategic positions. It can thus be concluded that adequately considering such nonlinear effects constitutes an important step to optimally exploit the economic value of UPHES units. However, even convexification or linearization procedures are intrinsically onerous computationally, which prevents them to consider the proper dynamics of the system (with an optimization step lower than 1 minute). Moreover, these techniques are also associated with modeling approximations that may lead to infeasible solutions.

To address these issue, we implement a hybrid procedure, which consists in the sequential operation of a simplified optimization tool and an advanced simulator, both included into a control loop ensuring the convergence towards a feasible and realistic solution. Although the convergence of the procedure cannot be theoretically guaranteed, the proposed iterative procedure has led to satisfactory results in the tested cases.

Overall, the proposed methodology enables to immunize the scheduling of UPHES against modeling inaccuracies used for approximating the nonlinear effects of the unit, thereby avoiding the associated market penalties for non-delivered energy. The model may thus be used as a decision tool in the UPHES daily scheduling, or may help regulators and system operators to better estimate the available flexibility from these new UPHES resources.

7. References

[1] J. I. Pérez-Diaz, M. Chazarra, J. Garcia-Gonzalez, G. Cavazzini and A. Stoppato, “Trends and challenges in the operation of pumped-storage hydropower plants,” Renewable and Sustainable Energy Reviews, vol. 44, pp. 767-784, 2015.
[2] SmartWater Pumped Hydro Storage, “Outcomes and Perspectives” in Cluster TWEED conference, May 2018.
[3] A. I. Wood and B. F. Wollenberg, “Power Generalion, Operafion and Control,” ed. New York: Jonh Wiley & Sons, 1984.
[4] O. Nilsson and D. Sjelvgren, “Mixed-integer programming applied to short-term planning of a hydro-thermal system,” *IEEE Trans. Power Syst.*, vol. 11, no. 1, pp. 281–286, Feb. 1996.
[5] A. Arce, T. Ohishi, and S. Soares, “Optimal dispatch of generating units of the Itaipu hydroelectric plant,” *IEEE Trans. Power Syst.*, vol. 17, no. 1, pp. 154–158, Feb. 2002.
[6] E. C. Finardi and E. L. da Silva, “Solving the hydro unit commitment problem via dual decomposition and sequential quadratic programming,” *IEEE Trans. Power Syst.*, vol. 21, no. 2, pp. 835–844, May 2006.
[7] J. P. S. Catalao, S. J. P. S. Mariano, V. M. F. Mendes and L. A. F. M. Ferreira, "Scheduling of Head-Sensitive Cascaded Hydro Systems: A Nonlinear Approach," *IEEE Trans. Power Syst.*, vol. 24, no. 1, pp. 337-346, Feb. 2009.
[8] A. J. Wood and B. F. Wollenberg, *Power Generation, Operation, and Control*. New York, NY, USA: Wiley, 1996.
[9] R. Naresh and J. Sharma, “Hydro system scheduling using ANN approach,” *IEEE Trans. Power Syst.*, vol. 15, no. 1, pp. 388–395, Feb. 2000.
[10] B. H. Yu, X. H. Yuan, and J. W. Wang, “Short-term hydro-thermal scheduling using particle swarm optimization

method," *Energy Convers.Manage.*, vol. 48, no. 7, pp. 1902–1908, Jul. 2007.
[11] X. Guan, A. Svoboda, and C.-A. Li, "Scheduling hydro power systems with restricted operating zones and discharge ramping constraints," *IEEE Trans. Power Syst.*, vol. 14, pp. 126–131, Feb. 1999.
[12] A. J. Conejo, J. M. Arroyo, J. Contreras and F. A. Villamor, "Self-scheduling of a hydro producer in a pool-based electricity market," *IEEE Trans. Power Syst.*, vol. 17, no. 4, pp. 1265-1272, Nov. 2002.
[13] A. Borghetti, C. D'Ambrosio, A. Lodi and S. Martello, "An MILP Approach for Short-Term Hydro Scheduling and Unit Commitment With Head-Dependent Reservoir," *IEEE Trans. Power Syst.*, vol. 23, no. 3, pp. 1115-1124, Aug. 2008.
[14] A. L. Diniz and M. E. P. Maceira, "A Four-Dimensional Model of Hydro Generation for the Short-Term Hydrothermal Dispatch Problem Considering Head and Spillage Effects," *IEEE Trans. Power Syst.*, vol. 23, no. 3, pp. 1298-1308, Aug. 2008.
[15] C. H. Chen, N. Chen and P. B. Luh, "Head Dependence of Pump-Storage-Unit Model Applied to Generation Scheduling," in *IEEE Trans. Power Syst.*, vol. 32, no. 4, pp. 2869-2877, July 2017.
[16] C. Cheng, J. Wang and X. Wu, "Hydro Unit Commitment With a Head-Sensitive Reservoir and Multiple Vibration Zones Using MILP," in *IEEE Trans. Power Syst.*, vol. 31, no. 6, pp. 4842-4852, Nov. 2016.
[17] B. Tong, Q. Zhai, and X. Guan, "An MILP based formulation for short term hydro generation scheduling with analysis of the linearization effects on solution feasibility," *IEEE Trans. Power Syst.*, vol. 28, no. 4, pp. 3588–3599, Nov. 2013.
[18] E. Pujades, P. Orban, S. Bodeux, P. Archambeau, S. Erpicum and A. Dassargues, "Underground pumped storage hydropower plants using open pit mines: How do groundwater exchanges influence the efficiency?" in Applied Energy, vol. 190, pp. 135-146, 2017.
[19] M. V. F. Pereira and L. M. V. G. Pinto, "Application of Decomposition Techniques to the Mid- and Short-Term Scheduling of Hydrothermal Systems," *IEEE Trans. Power App. and Syst.*, vol. PAS-102, no. 11, pp. 3611-3618, Nov. 1983.
[20] J. García-González, E. Parrilla, J. Barquín, J. Alonso, A. Sáiz-Chicharro and A. González, "Under-relaxed iterative procedure for feasible short-term scheduling of a hydro chain," in Proc. 2003 IEEE PowerTech Conference, vol. 2, Bologna, Italy, June 23–26, 2003.
[21] J.I. Pérez-Díaz, J.R. Wilhelmi and J.A. Sánchez-Fernández, "Short-term operation scheduling of a hydropower plant in the day-ahead electricity market," Electric Power Systems Research, vol. 80, no. 12, pp. 1535-1542, 2010.
[22] C. Revelle, "Optimizing Reservoir Resources: Including a new model for reservoir reliability". John Wiley & Sons, New York, 1999.
[23] M.T.L. Barros, F.T.C. Tsai, S.-L. Yang, J.E.G. Lopes and W.W.G. Yeh, "Optimization of large-scale hydropower system operations," ASCE Journal of Water Resources Planning and Management, vol. 129 (3), pp. 178–188, 2003.
[24] T. Mercier, J. Jomaux, E. De Jaeger, M. Olivier, "Provision of primary frequency control with variable-speed pumped-storage hydropower," in IEEE Powertech, Manchester, 2017.
[25] K. Bruninx, Y. Dvorkin, E. Delarue, H. Pandžić, W. D'haeseleer and D. S. Kirschen, "Coupling Pumped Hydro Energy Storage With Unit Commitment," in *IEEE Trans. Sust. Energy*, vol. 7, no. 2, pp. 786-796, April 2016.
[26] J.-F. Toubeau, J. Bottieau, F. Vallée and Z. De Grève, "Deep Learning-based Multivariate Probabilistic Forecasting for Short-Term Scheduling in Power Markets," *IEEE Trans. Power Syst.*, vol. 34, no. 2, pp. 1203-1215, March 2019.
[27] J.-F. Toubeau, J. Bottieau, F. Vallée and Z. De Grève, "Improved day-ahead predictions of load and renewable generation by optimally exploiting multi-scale dependencies," *IEEE ISGT-Asia*, pp. 1-5, Auckland, 2017.
[28] V. Dvorkin, S. Delikaraoglou and J. M. Morales, "Setting Reserve Requirements to Approximate the Efficiency of the Stochastic Dispatch," *IEEE Trans. Power Syst.*, vol. 34, no. 2, pp. 1524-1536, March 2019.
[29] A. Papavasiliou, S. S. Oren and R. P. O'Neill, "Reserve Requirements for Wind Power Integration: A Scenario-Based Stochastic Programming Framework," in *IEEE Trans. Power Syst.*, vol. 26, no. 4, pp. 2197-2206, Nov. 2011.
[30] J.-F. Toubeau, Z. De Grève, and F. Vallée, "Medium-Term Multi-Market Optimization for Virtual Power Plants: a Stochastic-Based Decision Environment," *IEEE Trans. Power Syst.*, vol. 33, no. 2, pp. 1399-1410, March 2018.
[31] A. B. T. Attya and T. Hartkopf, "Utilising stored wind energy by hydro-pumped storage to provide frequency support at high levels of wind energy penetration," in *IET Generation, Transmission & Distribution*, vol. 9, no. 12, pp. 1485-1497, 2015.
[32] A. Artiba, V.V. Emelyanov, S.I. Iassinovski, "Introduction to Intelligent Simulation: The RAO language," Operation Research & Decision Theory, Springer, 1998.
[33] A. Poulain, J.-R. de Dreuzy, P. Goderniaux, "Pump Hydro Energy Storage systems (PHES) in groundwater flooded quarries," Journal of Hydrology, vol. 559, pp. 1002-1012, April 2018.
[34] A. Arce, T. Ohishi, and S. Soares, "Optimal dispatch of generating units of the Itaipu hydroelectric plant," *IEEE Trans. Power Syst.*, vol. 17, no.1, pp. 154–158, Feb. 2002.
[35] A. Helseth, A. Gjelsvik, B. Mo and U. Linnet, "A model for optimal scheduling of hydro thermal systems including pumped-storage and wind power," in *IET Generation, Transmission & Distribution*, vol. 7, no. 12, pp. 1426-1434, Dec. 2013.
[36] M. Hupez, J.-F. Toubeau, Z. De Grève, and F. Vallée, "SARMA time series for microscopic electrical load modeling," Proc. ITISE 2016 Conf., pp. 354–365, 2016.

8. Acknowledgement

This work is being supported by Public Service of Wallonia (Belgium), within the framework of the Smartwater project.